In situ temperature measurements in microwave-heated gas-solid catalytic systems. Detection of hot spots and solid-fluid temperature gradients in the ethylene epoxidation reaction

Adrian Ramirez[a], *Jose L. Hueso*[a,b], *Reyes Mallada*[a,b]* *and Jesus Santamaria*[a,b]*

[a] Institute of Nanoscience of Aragon and Department of Chemical and Environmental Engineering, University of Zaragoza. C/Mariano Esquillor s/n, 50018 Zaragoza (Spain).

[b] Networking Research Center on Bioengineering, Biomaterials and Nanomedicine (CIBER-BBN), 28029, Madrid (Spain).

KEYWORDS: Microwave Heating, Thermographic Camera, Temperature Measurement, Temperature Gradient, Monoliths, Epoxidation, Ethylene

ABSTRACT. Infrared thermographic techniques have been used for the first time to determine real-time gas and solid temperatures, as well as gas-solid temperature gradients in microwave heated structured reactors. A special reactor vessel has been developed that allows direct observation of the catalyst under microwave heating, and an operating procedure is presented to obtain gas and solid apparent emissivities as a function of temperature. These values are thereafter used to calculate temperatures at any point in the gas and solid phases under reaction. The method has been used to obtain gas and solid temperatures during the ethylene epoxidation reaction carried out on a silver-copper oxide catalyst. The direct heating of the monolith walls produced a stable, large temperature gradient between the solid and the gas phase.

1. INTRODUCTION

The use of microwaves for heating dates back to the 1950s and was related to food processing applications[1]. Some of the advantages that we currently associate to microwave heating were already patent: fast, direct heating of the target materials compared to conventional heating mechanisms involving conduction, convection and radiation. Therefore, it could be rightly considered that the field of microwave-assisted chemical reactions dates back more than 60 years. However, the first specific studies of microwave-driven chemistry are typically dated in the 1970s and 1980s for inorganic and organic syntheses, respectively[2]. The field of chemical reactions under microwave (MW) heating has since expanded rapidly, with a myriad of potential applications that, in many cases, can be scaled up[3]. Of particular interest are microwave-assisted heterogeneous catalytic processes, both in liquid and gas phase, where the catalyst itself is preferentially heated by MW[4-7]. In this case, heat can be supplied directly to the catalyst, with a huge potential regarding energy savings. Microwave heating, often in combination with micro-reaction technology has also been heralded as a keystone of intensification in chemical processing[8-9].

Since the first studies of reactions under microwave irradiation a problem became apparent: due to the efficient energy delivery and fast heating afforded by microwaves, there was some uncertainty regarding the actual reaction temperature and the possibility of undetected hot spots. This problem has been found to be present even in liquid phase systems[10], where potential hot spots can be minimized thanks to the high heat removal capacity of the liquid. Thus in most cases, the so-called microwave effects (acceleration of chemical reactions compared to conventional heating) have been explained as thermal effects due to inhomogeneous heating of the liquid[11-12]. The problem becomes more severe in liquid phase catalyzed reactions where the

catalyst acts simultaneously as a MW absorber[4,13-14]. However, even in these cases temperature inhomogeneity can be reduced by introducing forced convection in the form of a fast stirring of the liquid mass[14]. On the other hand, in gas-solid systems the induction of hot spots in the microwave-absorbing solid phase (catalyst) becomes most likely. This is the result of several concurring factors: First, solid-fluid heat transfer coefficients are typically one order of magnitude lower when the fluid is a gas rather than a liquid. Second, the much lower density (and often also the lower heat capacity) of a gas implies that, to remove a certain amount of heat from a solid, the volume of gas needed is two to three orders of magnitude higher than in the case of a liquid. Finally, in most cases the solid catalyst in a microwave-heated reactor is static, meaning that stirring to achieve homogeneity is not an option.

The microwave heating mechanism in solids is often complex and varies depending on the solid nature. Nevertheless, the heating can always be described in terms of the dielectric properties of the material: dielectric constant (ε'), dielectric loss (ε'') and the loss tangent (δ), which is the ratio of ε'' and ε' [15]. The dielectric constant (ε') represents the penetration of the microwave radiation inside the material while the dielectric loss (ε'') refers to the capacity of the material to dissipate the radiation in the form of heat. Thus, a material with high loss tangent (δ) is always desirable for efficient MW heating, as a too high dielectric constant (ε') implies that the material is nearly transparent to microwave radiation.

From the above it is clear that in gas-solid systems a fast MW heating of the solid (catalyst/support) phase is likely to lead to i) the formation of hot spots in the solid and ii) significant gas-solid temperature gradients. Obviously, knowing the temperature of the gas and solid phases and ensuring sufficient homogeneity of catalyst temperature are essential requirements for any study of catalyst performance under microwave heating. As it has been

noted[7], in microwave-driven gas phase catalysis, because of defective temperature measurements "different effects are often observed and contradictory conclusions are drawn". Indeed, hot spots can be responsible for apparent increments of the reaction rates, equilibrium shifts, and changes in product selectivities.

Because of the difficulties involved, temperature measurements in microwave-heated reactors is a topic often discussed in the literature. Different overviews (see for instance Stankiewicz et al.[16], Kappe[10]) discuss the challenges involved and present examples where serious errors in temperature measurement are possible. The main problems in temperature measurements under microwave heating can be summarized as follows: (i) Conventional means, such as thermocouples or mercury thermometers, cannot be used as they could couple with the electromagnetic field and create interferences or even produce sparks. Since a conventional thermocouple may interfere with the MW field, in some works the temperature was estimated by turning off the MW power and quickly introducing a thermocouple in the bed[17] through a quartz thermocouple sheath. Then temperature readings were obtained and the bed temperature could be obtained by extrapolating to zero time, although with significant uncertainties related to the temperature measurement delay; (ii) External infrared (IR) sensors are customarily built-in in commercial monomodal microwave units but can only measure the temperature at the external surface of the reaction vessel, a value that may deviate strongly from the internal temperature, even for liquid systems[10]. With an external infrared (thermography) camera a larger number of temperature measurement points are possible with good spatial resolution depending on the camera optics, but the problem remains the same: only temperatures at the external wall can be read; (iii) Fiber optic (FO) measurements on the other hand can give accurate temperature readings inside the reaction vessel and are immune to interference by microwaves. However, the

measurement is only local, and not suitable for the detection of hot spots, given the steep temperature profiles that often develop under MW heating.

Stankiewicz and co-workers[7] alleviated this problem by introducing the optical fiber inside a quartz well, allowing displacement of the measuring probe along the bed. While this procedure helps in the detection of higher temperature zones, it presents the disadvantage of introducing delays in temperature measurements and inaccuracies due to the heat transfer resistance of the quartz well. In summary, accurate temperature measurements in gas-solid catalytic reactors under microwave heating remains as an open challenge and this represents a very significant hurdle in the developing of microwave-heated reactors, a highly promising field.

Recently in our group[18-19], a dual-measurement system was implemented to follow the temperature of gas and solid in a structured reactor under microwave heating. On the one hand, a thermographic camera was used outside the reactor but, instead of measuring the outside wall temperature, a partially transparent IR window was used to monitor the temperature of a microwave-absorbing, catalyst-coated monolith, after appropriate calibration. In this way, the average solid temperature could be obtained, and the monolith was directly monitored for the presence of any hot spots or temperature in-homogeneities. On the other hand, an optical fiber was located a couple of mm downstream of the monolith to have a direct measurement of the *average* temperature of the gas exiting the monolith. In spite of its limitation (only one temperature measuring point for the gas was implemented) this method provided for the first time an experimental assessment of the gas-solid temperature gap under microwave heating, which was estimated at 50-60 K for the conditions used in that work[19]. Similar combinations of IR techniques with IR transparent windows have already been used in the literature to measure

temperatures in heterogeneous catalytic systems and to determine the enthalpy of fast exothermic reactions[20-21].

This work has the ambitious objective of measuring the gas temperature in the channels of a cordierite monolith coated with a silver-copper oxide catalyst during the ethylene epoxidation reaction, while simultaneously measuring the temperature of the solid surface. To this end, we will make use of the fact that gases that present absorption and emission in the infrared range (there are many examples, including water, CO_2 or ethylene) can be detected with a thermographic camera. The procedure is well known and in fact is currently used for the detection of leaks in industrial pipes[22-23]. Matters, however, get much more complex when the temperature of a gas has to be determined by measuring through a partially transparent window and through different atmospheres, plus the interference of any surfaces in view within the optical path. We have designed a new experimental set up to facilitate direct real-time temperature observation and we have also developed a calculation algorithm that allows us to obtain the temperature of both the monolith surface and the gas located in the channels. The procedure has been demonstrated by obtaining gas and solid temperatures under microwave heating during the ethylene epoxidation reaction.

2. EXPERIMENTAL SECTION

2.1 Chemicals and Equipments

Copper nitrate ($Cu(NO_3)_2 \cdot 3H_2O$, 99%, Aldrich), silver nitrate ($AgNO_3$, 99 %, Aldrich), sodium hydroxide (NaOH, Aldrich), and ethanol (EtOH, 96 %, Aldrich) were all used as received.

Temperatures were registered using a thermography camera and an optical fiber. The thermographic camera is a NEC InfRec R300RS which operates in the range of 8 to 14 μm and

allows temperature measurement between -40 ºC and +500 ºC. The sensitivity of the camera is 0.03 °C with a frequency of 60 Hz and a spatial resolution of 1.2 mrad. The fiber optic is a Neoptix fiber optic sensor (temperature range -270 to +250 ºC) connected to a multichannel fiber optic signal conditioner Neoptix™ Reflex™. The temperatures were continuously measured and recorded using commercial software. Scanning electron microscopy (SEM) analysis was carried out with a FEI-Inspect S50 equipment. Preliminary electron microscopy observations were completed with a T20–FEI microscope with a LaB_6 electron source fitted with a "SuperTwin®" objective lens allowing a point to point resolution of 2.4 Å. Aberration corrected scanning transmission electron microscopy images were acquired using a high angle annular dark field detector in a FEI XFEG TITAN electron microscope operated at 300 kV equipped with a CETCOR Cs-probe corrector from CEOS Company allowing forming an electron probe of 0.08 nm. The geometric aberrations of the probe-forming system were controlled to allow a beam convergence of 24.7 mrad half-angle to be selected. Elemental analysis was carried out with EDS (EDAX) detector which allows performing EDX experiments in scanning mode.

2.2 Monolith preparation

The preparation of catalyst-coated monoliths was done according to our recent work[19]. Briefly, cordierite monoliths with 1 mm square channels were cut into cylinders with 12 mm diameter and 15 mm length. Cordierite monoliths are commonly used as catalyst supports. In this case, this material was also selected due to the fact that cordierite is largely microwave-transparent; because of this, the microwave energy is mainly absorbed by the Ag/CuO catalyst. The preparation of the microwave-absorbing silver-copper oxide catalyst used for ethylene epoxidation followed previously reported methods in our laboratory[19 ,25]. Catalyst loading was carried out by controlled immersion of the monoliths in ethanolic suspensions (1.5 g of catalyst

in 50 mL) inside an ultrasonic bath for 30 minutes followed by calcination (2 h) at 250 ºC. This process was repeated several times until the desired catalyst loading was achieved (ca. 10 wt %).

2.3 Emissivity calibration

Knowing the emissivity of the materials employed is critical in temperature measurements by IR thermography. Because of this, the emissivity of the catalyst-loaded monolith was determined as a function of temperature employing two different techniques. First, the monolith was introduced in a convection oven and the temperature was allowed to equilibrate (at 100, 150 and 200 ºC). The temperature was then measured with the thermographic camera, adjusting the emissivity to obtain a reading corresponding to the known, steady state temperature of the oven. In a second procedure, the monolith was introduced in the monomodal microwave cavity with an optical fiber inserted tightly in the central channel of the monolith as a temperature reference. The power of the MW generator was adjusted to achieve temperatures of 100, 150 and 200 ºC in the fiber. Then, the temperature of the monolith walls next to the fiber (which were assumed to be at the same temperature) was measured with the infrared camera, adjusting the emissivity of the monolith to read the same temperature as the fiber. Very similar emissivity values were obtained by both methods. Conveniently, the values given below are those obtained in the microwave cavity with the optical fiber placed centrally on the monolith. The validation of the optical fiber reading was also checked (see Figures S1 and S2) by comparing the readings of the fiber with the temperature measurements of the IR camera at the closest surface locations, using the emissivity obtained in the previous calibration experiments. The temperature differences between the optical fiber and the IR camera readings were lower than 0.5ºC.

2.4 Microwave heating and temperature measurements

The experimental set-up is described in Figure 1. Microwave-induced heating was addressed in a TE510 monomodal cavity equipped with a magnetron generator operating at 2.45 GHz (maximum power 300 W). The cavity was adjusted to reduce the reflected power thanks to a moveable short circuit. MW heated directly the Ag/CuO catalyst deposited on the cordierite monolith, since the cordierite is largely microwave-transparent.

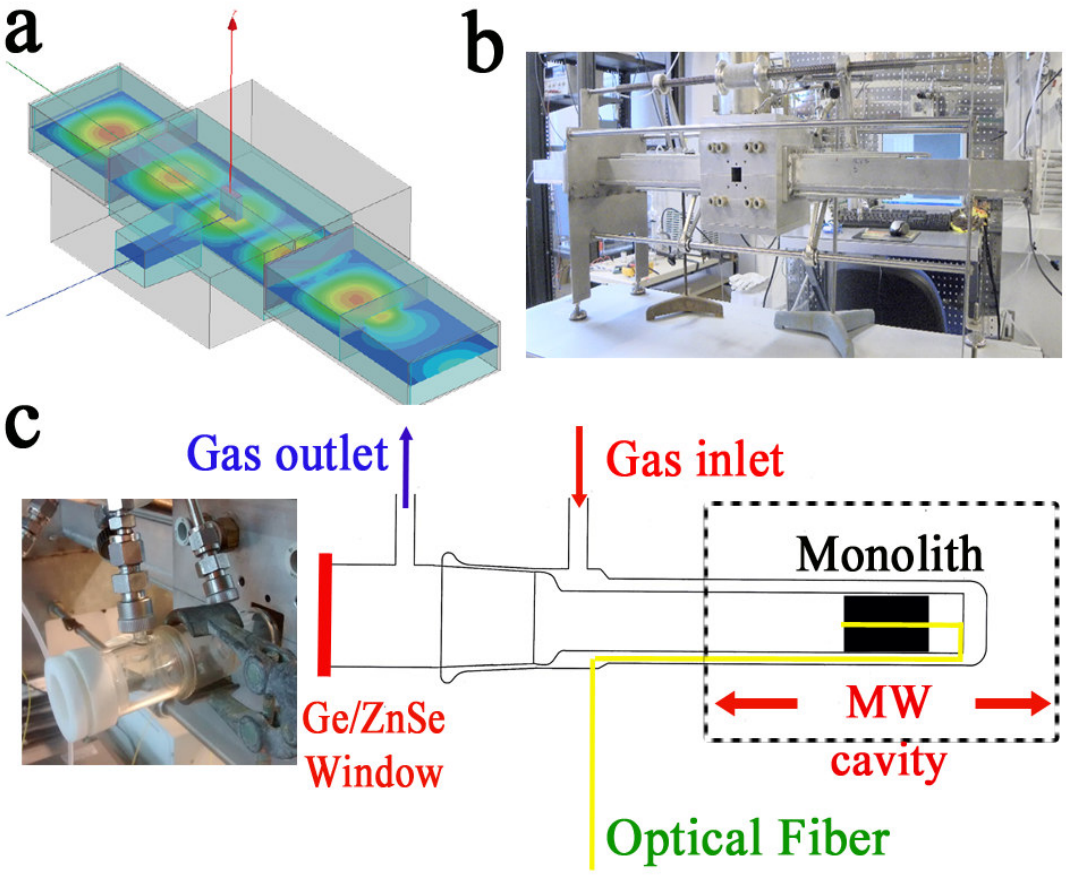

Figure 1. Microwave Reactor: a) Simulated electric field distribution in the monomodal MW cavity; b) Digital photograph of the MW cavity; c) Digital image of the custom-designed quartz reactor vessel protruding outside the MW cavity and detailed sketch of the different parts of the quartz vessel including the gas inlet and outlet, the filter windows (Ge or ZnSe), the optical fiber and the catalytic monolith.

The monolith (Figure 1c) was placed inside a quartz vessel, introduced in the microwave cavity, at a nodal position where the electric field reaches a maximum. This quartz vessel was

purposely designed to hold the monolith and fit in the monomodal cavity while allowing temperature measurements under reaction conditions. It consists of two concentric frosted quartz tubes with a 3 cm observation window replacing the quartz top (Figure 1c). The windows employed were made of either ZnSe (provided by Crystaltechno Ltd) with an infrared transparency of 80% in the camera range (8 – 14 μm), or Ge with a specific coating (provided by Alkor Technologies) having an infrared transparency of 80% in the main ethylene emission range (10 – 11 μm, see Figure 2b). The gas feed (6% ethylene, 12% oxygen and 82% helium) was introduced from the outer tube flows through the monolith channels and leaves through the inner tube outlet (Figure 1c). As explained, the temperature was simultaneously measured with an optical fiber placed in the central channel of the monolith and with a thermographic camera through the ZnSe or Ge windows (Figure 1c). The reading of the optical fiber was always used as a reference and the emissivity of the camera was adjusted to obtain this value of temperature in the monolith surfaces close to the optical fiber. To assess any errors due to radial temperature gradients independent emissivity measurements were carried out in at least 5 different locations at the monolith surface, as close as possible to the optical fiber. The average deviation was lower than 5%. The monolith temperature was increased from 100 to 200 °C in steps of 50 °C, varying the microwave power. The flow rate was set to obtain a WHSV of 0.2 L min^{-1} g_{cat}^{-1}. For conventional heating, the same quartz holder was placed inside an electrical oven. Temperature profiles were measured with a thermocouple located in the same position as the optical fibers and connected to a PID controlled electrical furnace to maintain the desired temperature.

3. TEMPERATURE ESTIMATIONS USING INFRARED THERMOGRAPHY

The operational principle behind infrared cameras is based on the fact that all bodies at temperatures above 0 K emit electromagnetic radiation, being the intensity of this radiation dependent on the temperature and the wavelength considered. The infrared camera detectors measure the amount of radiation from an object and translate it into temperature using the Stefan–Boltzmann law, which gives the radiation flux emitted by a surface as a function of temperature:

$$J = \varepsilon \cdot \sigma \cdot T^4 \qquad (Equation\ 1)$$

where T is the temperature (K), is the Stefan–Boltzmann constant (5.6 x 10^{-8} m^{-2} K^{-4}) and • is the object emissivity, expressed as the ratio between the radiant energy emitted by the object and that of a blackbody would at that same temperature. A blackbody emits 100% of the energy it absorbs and has an emissivity of 1. The strong dependence of J with temperature (T^4) implies that, in a target where there are large temperature variations, only those regions with the highest temperature will make a significant contribution to the radiation flux. The emissivity of a surface changes with temperature[26], and its value must be precisely known to acquire accurate temperatures with a thermal camera. Incorrect emissivity values may lead to large temperature deviations, given the exponential dependency in the Stephan–Boltzmann's Law.

The medium where the infrared measurements are carried must also be considered in order to obtain accurate measurements. In many works the medium is considered transparent, implying that the gases in the optical path neither absorb nor emit radiation in the observation range (IR) and therefore do not affect the camera readings, but this is often not the case. Thus, gases such as CO, NO, CO_2, SO_2, H_2O and many hydrocarbons present significant absorption bands in the infrared range, due to vibrational and rotational motions[24]. Each molecule has a specific absorption range within the infrared spectrum and IR cameras can detect the absorptive and

emissive characteristics of these gas molecules. When the detection range of the IR camera can be tuned to a narrow spectral region where the target molecules display a strong absorption, then the gas can be visualized[22], i.e., in this case the gas influence will not be negligible, and this provides a basis to determine the gas temperature. For this, the emission and absorption characteristics of the gas cloud must be known, at the operation temperatures of interest.

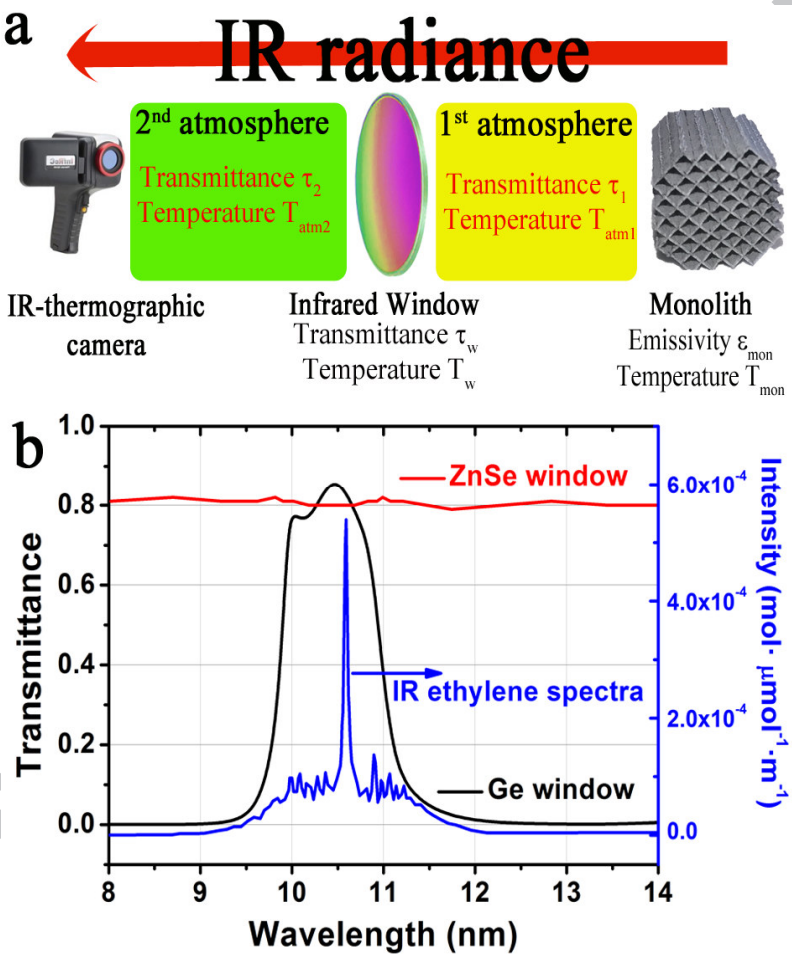

Figure 2. a) Schematic representation of the different factors under evaluation that can influence the readings of the thermographic camera. b) Left axis: IR transmittance of the employed Ge and ZnSe windows; Right axis: Infrared spectra of ethylene, adapted from Ref[27].

There are two well established methods to determine the emissivity of a gas: the total energy method[28] and the absorption band model[29]. In the band absorption method, the total emissivity (or

just emissivity) is obtained by adding up the monochromatic emissivity (i.e., the emissivity at a certain wavelength) from all the bands that give a significant contribution to the total radiation emitted. The emissivity of a gas is usually lower than the emissivity of a solid object as gases only absorb and emit in certain wavelengths, with each absorption/emission feature in a spectrum corresponding to a specific excitation of the molecule. The main absorption bands of ethylene are in the range of 10 to 11μm and can be detected by most commercial infrared cameras that usually operate in the 8 to 14 μm range (see Figure 2b). However, ethylene is nearly transparent in the 8 to 10 and 10 to 14 μm ranges. Since the camera receives radiation from other objects in that wavelength range, the ethylene contribution to the total radiance received is generally low, and the reading loses accuracy. This problem can be alleviated by employing an optical filter (e.g. a Ge window) that blocks undesired wavelengths, leading to a more selective reading in the bands corresponding to the target gas.

Figure 2a summarizes the factors affecting the radiance received by the camera when a semi-transparent window is placed between the object (in our case a coated monolith immersed in an ethylene-rich atmosphere), a second atmosphere (ambient air) and the camera. There are six main contributions[30]:

1. The radiance emitted by the object, which is affected by the first atmosphere, the transmittance of the window, and finally the second atmosphere.
2. The radiance reflected by the object that is affected by the transmittance of the window and the first and second atmospheres.
3. The radiance emitted by the first atmosphere, which is then affected by the transmittance of the window and the second atmosphere.
4. The radiance emitted by the window, affected by the second atmosphere.

5. The radiance reflected by the window's outer surface, affected by the second atmosphere.
6. The radiance contribution of the emitting second atmosphere.

In our case only components 1 and 3 have significant contributions. Component 2 is neglected against components 1 and 3 since the camera detector is placed at the same height of the object (the coated monolith, see Figure 1c) and aligned with the optical path, where the contributions of 1 and 3 are highest[31]. The window and the outside (second) atmosphere are at room temperature. Given the strong temperature dependency of the Stefan-Boltzmann and Planck laws, the emission of both is negligible compared to the emission of the object and of the inner atmosphere, and therefore components 4 to 6 can be neglected. It should also be considered that the first atmosphere in our case is ambient air, with a relatively low concentration of absorbing gases (CO_2, H_2O) and a short optical path, therefore its transmittance is close to 100%. With the above assumptions we can approximate the radiance reaching the camera as that from the monolith (through the first atmosphere and the window) plus that from the first atmosphere (including the gas inside the monolith channels), through the window. The relative strength of each contribution depends on the gas temperature[32]. When the gas temperature is significantly lower than that of the object (as would likely be the case when the solid is directly heated by MWs) the contribution of component 3 can be neglected due to the dependency of the radiance with temperature (see below). However, a colder gas cloud is still able to absorb radiation and therefore leads to a decrease of the object signal. The attenuation losses of IR radiation passing through a gas can be obtained from Bouguer's law:

$$I(\lambda) = I_0(\lambda) \cdot e^{-\tau(\lambda,C,L)} \qquad (Equation\ 2)$$

Where I_0 is the radiance emitted by the object, I the radiance reaching the receptor and is the optical depth of the gas, which depends on wavelength ( ), gas concentration (C), and length of the optical path through the gas (L). On the other hand, when the gas is at similar or higher temperature than the object, component 3 cannot be neglected. If the camera detector range is tuned to be sensitive to that spectral region, then the gas contribution adds to the object radiation regarding the total radiance received by the camera. The radiance emitted by the hot gas cloud will follow the Planck's law which describes the electromagnetic radiation emitted by a black body:

$$I(\nu, T) = \frac{2 \cdot h \cdot \nu^3}{c^2} \cdot \frac{1}{e^{\frac{h \cdot \nu}{k \cdot T}} - 1} \qquad (Equation\ 3)$$

Where h is the Planck constant, c is the speed of light in a vacuum, k is the Boltzmann constant, is the frequency of the electromagnetic radiation and T is the absolute temperature of the body.

Next we will show how, by selecting the appropriate materials for the observation windows and by studying the system under both microwave heating (where the solid monolith is selectively heated) and conventional heating (were both the monolith and gas in the monolith channels are roughly at the same temperature), we can estimate the temperature gradient between the gas and the Ag/CuO solid during the reaction of ethylene epoxidation under microwave heating.

4. RESULTS AND DISCUSSION

4.1 Catalytic monolith characterization

Figure 3a shows the macroscopic appearance of the cordierite monolith after successive deposition and calcination steps to obtain a 10% wt. loading of the microwave-sensitive

(Ag/CuO) catalyst[19,25]. A closer look by SEM and TEM analysis shows a homogeneous distribution of the catalyst along the monolith channels (Figure 3b) and the tubular-shaped morphology of the nanostructured hybrid with average lengths of up to 1 micron and widths below 200 nm (Figures 3c-3d). A more detailed analysis by HAADF-STEM combined with EDS mappings (Figures 3f-3g) reveals the clear intertwining of both silver and copper oxide phases and the distribution of the metallic phase either as segregated nanoislands or as anisotropic inner structures (Figures 3e-3g)[25]. Prior to the reaction tests, temperature measurements were carried out under microwave heating with the monolith outside the reactor (in ambient air), and thermography images were acquired in order to evaluate the homogeneity of monolith heating.

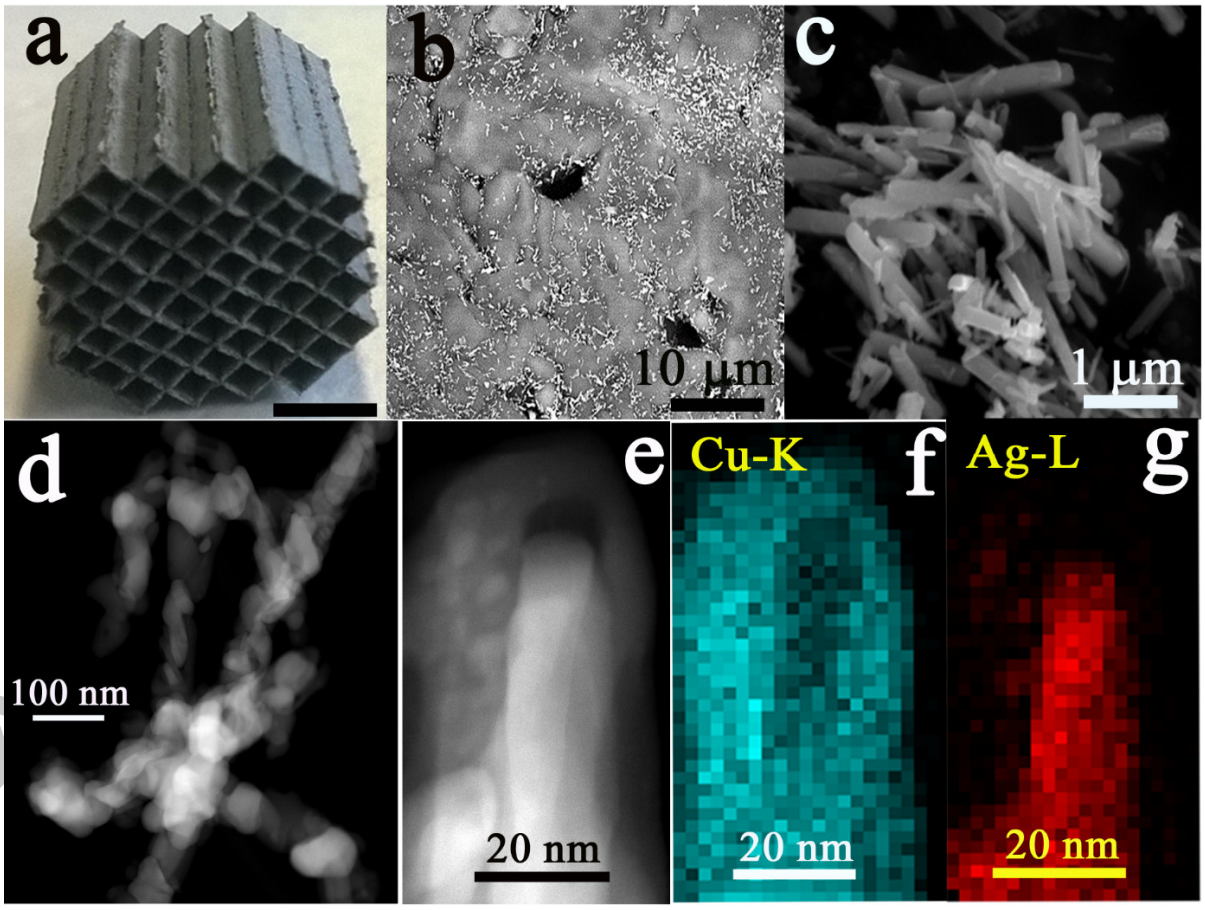

Figure 3. a) Digital photograph of a cordierite monolith after the deposition of the Ag-CuO catalyst by successive sonication and calcination steps for a 10% wt. loading; b) Low-magnified SEM image accounting for the

homogeneous distribution of the catalyst along the monolith channels; c) Magnified SEM image of the Ag-CuO catalyst; d) HAADF-STEM image corresponding to the Ag-CuO tubular-shaped catalyst; e)-g) STEM image and the corresponding EDS mapping analysis of the Cu-K and Ag-L edges, respectively.

Figure 4 shows that the homogeneity of the heating largely depends on the distribution of the microwave-absorbing catalyst. Thus, a non-homogeneous load leads to pronounced temperature differences, while an optimized, even distribution gives a rather uniform heating (in the case of the figure, maximum temperature deviations of less than ± 10 ºC). It must be taken into account that the pictures were taken in stagnant air, with direct (i.e., no interposed window) observation of the monolith under MW heating. Under reaction with flow in the monolith channels, temperatures are expected to be even more homogeneous thanks to convection heat transfer. Achieving a homogenous heating in the central volume of the monolith is very important, as will be shown below, since the temperature measured by an optical fiber inserted in the central channels is taken as a reference in the algorithm developed to calculate temperatures.

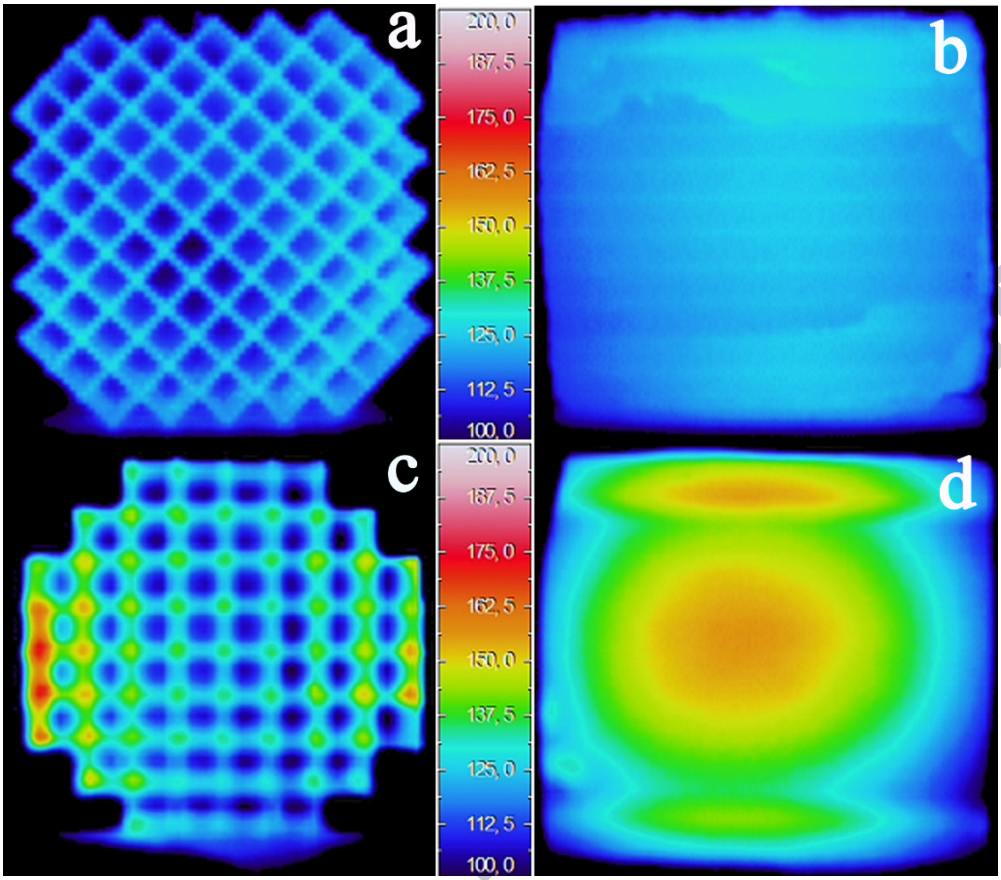

Figure 4. Thermal images acquired for a monolith coated with the microwave-absorbing Ag/CuO catalyst (10% wt. loading). a) Front view of a homogeneously coated monolith; b) Side view of a homogeneously coated monolith; c) Front view of a monolith with uneven catalyst distribution; d) Side view of the monolith with uneven catalyst distribution. Emissivity adjusted to 0.8; MW power = 20 W; Thermal scale ranges between 100 and 200 ºC.

4.2 Apparent emissivity measurements

Figure 5 shows thermal images of a coated monolith under MW heating, placed inside the reaction vessel and viewed through a ZnSe window at an average temperature around 150 ºC. Either the reaction mixture (Figure 5a) or helium flowed through the system (Figure 5c). The central part of the monolith is occupied by an optical fiber that has a different emissivity than the monolith and thus appears to be at a different temperature. The lumen of the channels also appears darker, occupied by the gas, with a different emissivity. The objective in this case is to obtain from the thermal image of the camera a reading that corresponds to the temperature of the

monolith surface. To this end, as already explained, the apparent emissivity of the monolith material is adjusted to obtain, in the points closer to the optical fiber, a temperature reading that corresponds to the true temperature measured by the optical fiber. The emissivity value obtained is an *apparent emissivity*, since the monolith is not observed directly, but through i) the ZnSe window and ii) the optical path that runs through the 1st atmosphere, occupied by either helium or the reaction mixture. The apparent monolith emissivity decreases from the value close to 0.80 that was obtained under direct observation (no window, no absorbing atmosphere) to 0.60 in helium (reduction due to the effect of the ZnSe window) and to 0.45 in the reaction atmosphere (combined effect of the ZnSe window and the absorbing gases in the vessel). The difference between the emissivity in Figures 5a and 5c implies that the gas in the first atmosphere (between the window and the monolith) absorbs infrared radiation which is mainly due to the presence of ethylene, see Figure 2. The lower radiance received by the camera detector when the atmosphere contains the reaction mixture (as a consequence of the absorption by ethylene in the range of 10 to 11 μm) is accounted for by a decrease in the apparent emissivity. With this corrected value of emissivity a good approximation to temperatures in the monolith surface can be obtained. It is interesting to note that the maximum temperature deviations across the monolith have now been reduced from ± 10 ºC (in stagnant air) to ± 5 ºC due to increased heat transfer by convection caused by the gas flowing through the channels (Figures 5b, 5d).

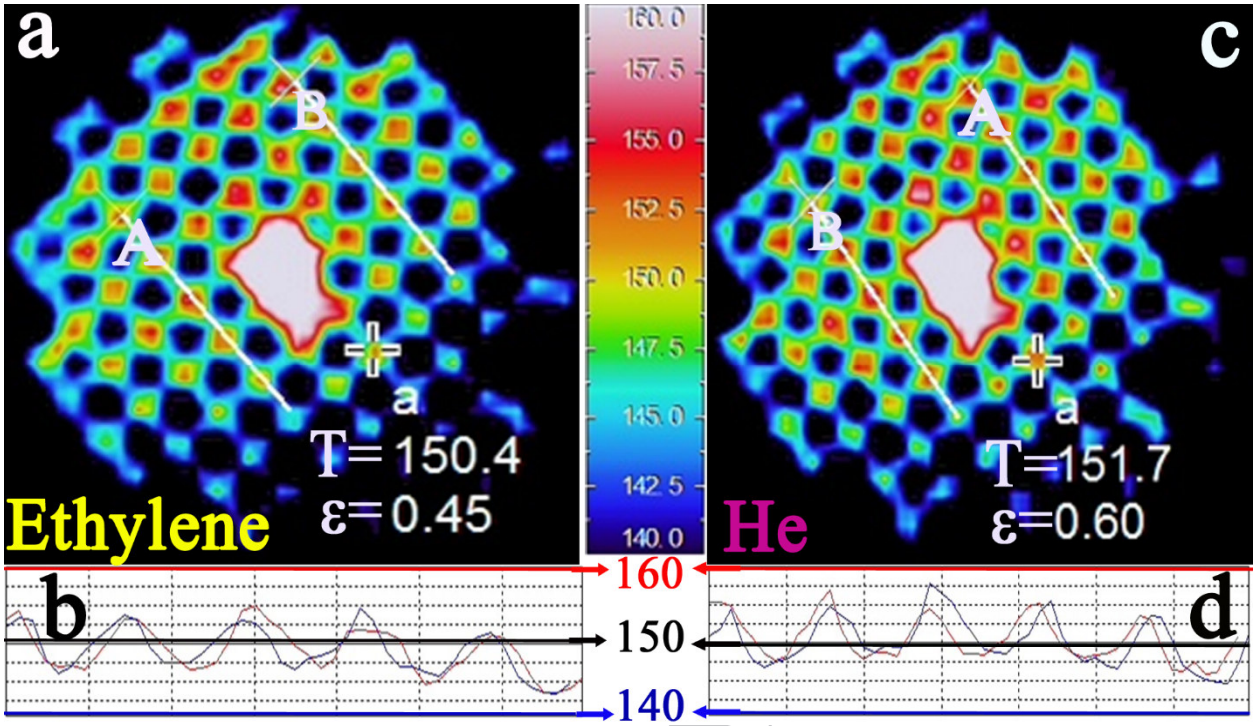

Figure 5. Thermal images of a coated monolith under MW heating in the reaction vessel seen through a ZnSe window at 150 ºC (thermal scale ranges from 140 to 160 ºC): a)-c) In the presence of the reaction mixture containing ethylene and He, respectively; b)-d) Temperature profiles readings following the lines labeled as A and B along the monoliths depicted in Figures a)-c). Note that the apparent higher temperature of the optical fiber placed in the central channel is an artifact caused by the difference in the emissivity between the fiber optic and the cordierite monolith.

Figure 6 compares thermal images of the same catalyst-coated monolith through different windows (ZnSe or Ge) and under different types of heating (MW and conventional). It can be observed than under MW heating the temperature profiles are similar for both windows (Figures 6a, 6b), with a clear temperature difference between the monolith wall and the channel lumen. For the same solid temperature, under MW heating the solid is heated directly, and the gas in the channels is comparatively cooler[19]. Therefore, the influence of the gas cloud in the optical path between the window and the monolith is diminished and the monolith structure can still be seen

with either window. However, under conventional heating the temperature profiles are radically different (Figures 6c, 6d).

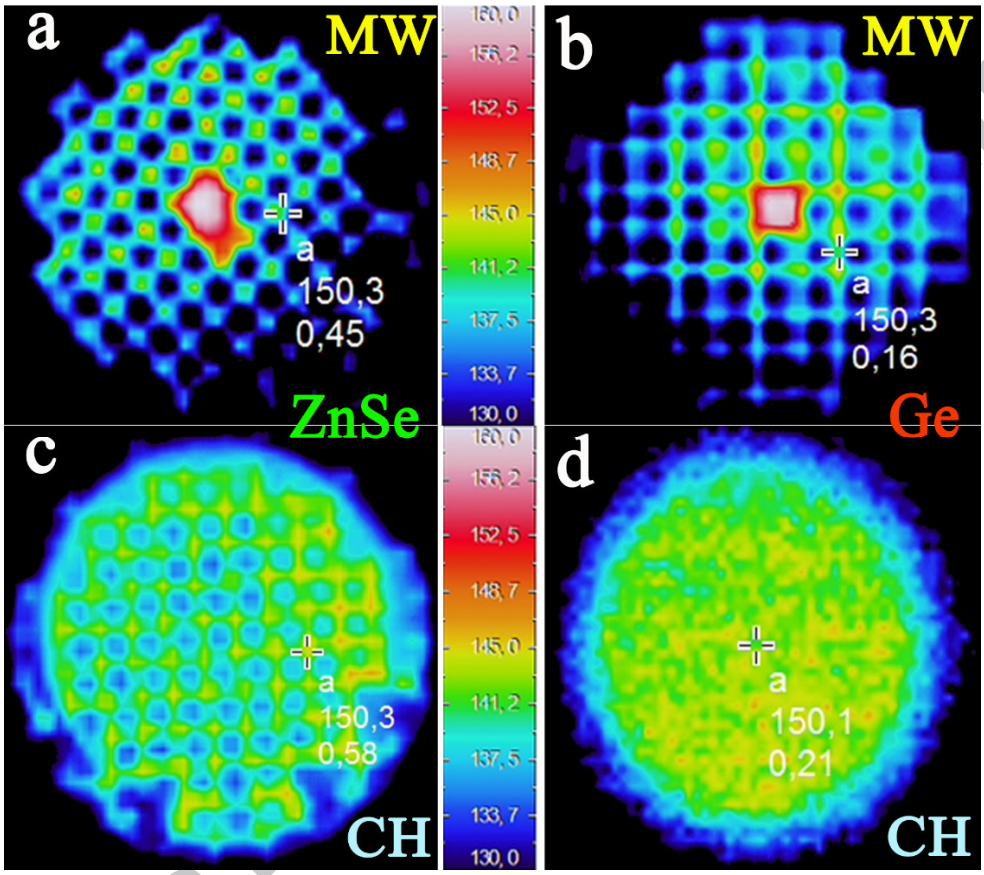

Figure 6. Thermal images of the coated monolith inside the reaction vessel, under conventional and MW heating. The monolith was heated to approximately 150 ºC in the reaction mixture (temperature measured by the optical fiber). The thermal scale ranges from 130 to 160 ºC; a) MW-induced heating using the ZnSe window; b) MW-induced heating using the Ge window; c) Conventional heating in the presence of the ZnSe window; d) Conventional heating using the Ge window.

The boundary between the monolith and the channels becomes blurred to the point that it is not possible to observe the monolith channels through the Ge window (Figure 6d). The hot ethylene cloud now becomes a major contributor thanks to the Ge window that blocks radiation in the ranges of 8 to 10 µm and 10 to 14 µm (thereby increasing the relative contribution of ethylene),

while the ZnSe windows allows the transmission of radiation in the whole 8 to 14 μm range. The narrower detection range allowed by the Ge window maximizes the contribution of ethylene gas, and component 3 now prevails over component 1.

The variation with temperature of the apparent emissivity of the catalyst-coated cordierite monolith under microwave heating is given in figure 7a, for different observation windows and gas compositions of the 1st atmosphere. In agreement with the previous discussion, the lowest values of apparent emissivity are always obtained when the monolith is observed through the ethylene-containing atmosphere and the Ge window. With the same system, it is possible to obtain the apparent emissivity of the reaction atmosphere, when observation conditions are chosen in such a way that the relative contribution of component 3 prevails. This is achieved in our case when the monolith is conventionally heated and the temperature is read through the Ge window (see Figure 6d). The apparent emissivity is then adjusted to make the temperature reading coincident with the true gas temperature, read by a thermocouple or an optical fiber (conventional or MW heating). The apparent emissivity values are given in Figure 7b. The absence of artifacts was guaranteed by the fact that the same temperature-emissivity correlation was obtained when the experiment was run without a monolith, by simply observing the reaction chamber filled with the reactor gas feed through the Ge window, even though in this case there was no ethylene conversion. The fact that the same emissivity values for the reaction atmosphere at a given temperature were obtained irrespective of the conversion (at least up to 10% conversion) can be explained in this case by the similar the absorptive and emissive IR characteristics of the reactant (ethylene) and of the main product (ethylene oxide). This is a particular result for the ethylene oxidation reaction system within the IR range observed. For other reaction systems, the variation of the apparent emissivity of the reaction atmosphere (1st

atmosphere) would have to be obtained not only as a function of temperature, but also for different gas compositions, i.e. for different reactant conversions.

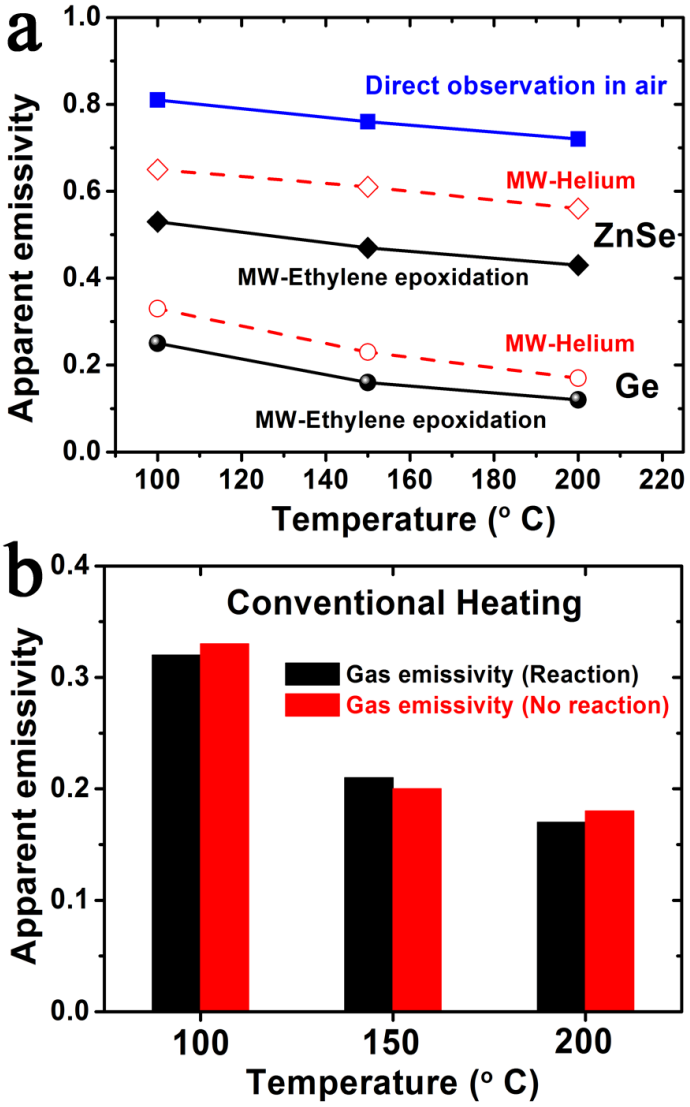

Figure 7. Variation of the apparent emissivity with temperature, depending on the measurement conditions. a) Emissivity of the coated monolith emissivity viewed through different windows and compositions of the 1st atmosphere. b) Emissivity of the reaction gas viewed through the Ge window (black bars: data obtained in the presence of the catalytic monolith, under conventional heating and reaction, red bars: data obtained on an empty reactor, filled with feed gas 6% ethylene, 12% oxygen and 82% helium, conventional heating, no catalyst, no reaction,).

4.3 Calculation of gas-solid temperature differences

Once the variation of apparent emissivity with temperature has been obtained for both the gas and the solid (monolith surface) under a given set of conditions (observation temperature and composition of the 1st gas atmosphere), the point temperatures at any location (gas or solid phase) can be obtained by a simple iteration procedure. The general calculation procedure is presented in Scheme 1.

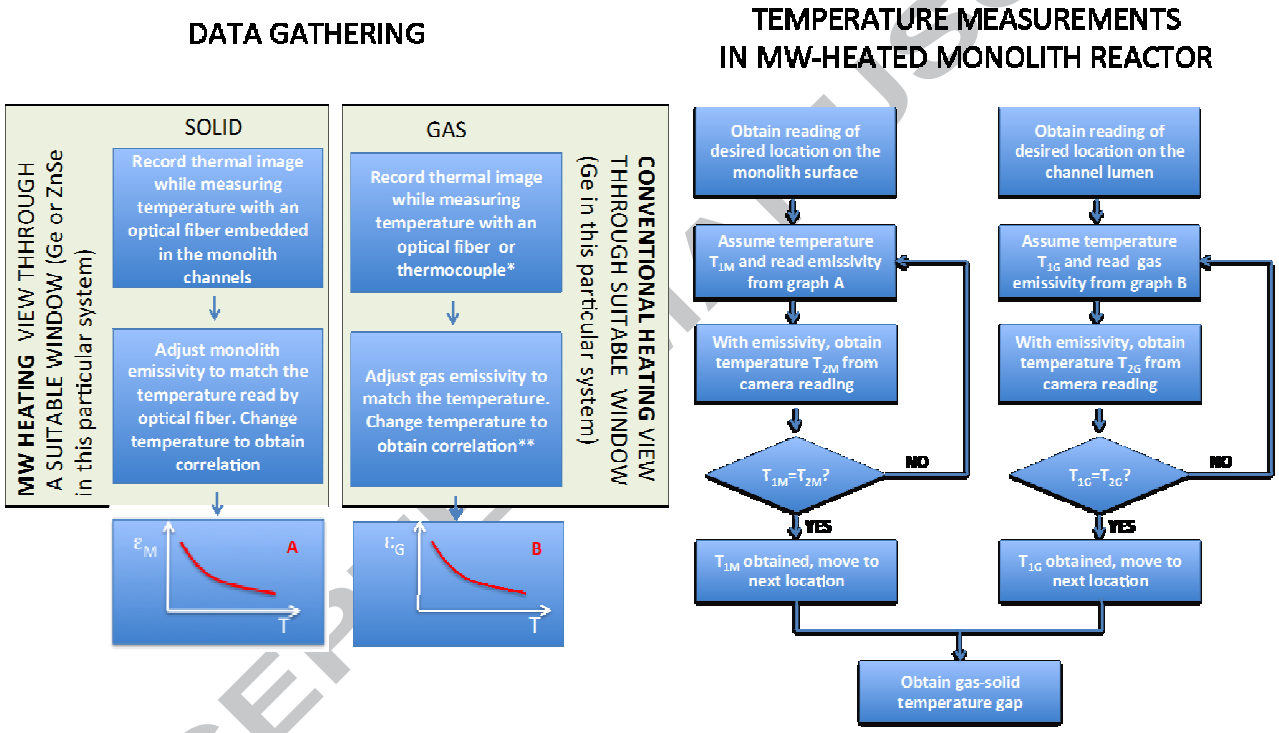

Scheme 1. Algorithm to obtain gas and solid temperatures and gas-solid temperature gradients during reaction under microwave heating. The data gathering step allows to obtain the necessary emissivity-temperature correlations before actual measurements. Notes: *Can be obtained with monolith in place if component 3 prevails, otherwise measurements should be done with chamber filled with gas only. **Different correlations may be needed for different gas compositions if there is a strong dependence of e with conversion

The results of the calculations following Scheme 1 for a specific case are illustrated in Figure 8, where thermal images for the monolith surface (Figure 8a) and the gas in the lumen of several monolith channels (Figure 8b) taken through a Ge window are shown separately, then merged in a single image (Figure 8c). Once the corrected emissivity values for gas and solid as a function of temperature are available, gas and solid temperatures throughout the reactor can be obtained from these images. In our case, these temperatures have been used to obtain the average solid-gas temperature gradient under microwave heating. The results are presented in Figure 8d, where the average solid-gas temperature gradient has also been estimated using two other alternative methods: i) solid temperature measured with an optical fiber inserted in the central monolith channel and exit gas temperature measured by an optical fiber close (1.5 mm) to the downstream monolith surface; ii) gas and solid temperatures measured using the procedure in Scheme 1, but using ZnSe windows. This procedure is thought to be less accurate than using the Ge windows, since in this case some contribution from the monolith may reach the camera, even if the point of measurement is selected in the lumen of the channels. It can be observed that the three methods gave values of the gas-solid temperature gradient in a similar range, 18 to 25 ºC at 150 ºC, 29 to 41 ºC at 150 ºC, and 47 to 58 ºC at 200 ºC. As could be expected, the gradient measured with the optical fibers is the largest since the temperature difference is measured between the fiber in the central channel (therefore the hottest location in the monolith) and the fiber 1.5 mm downstream. An even better agreement would be obtained by extrapolating optical fiber readings as a function of distance (see Figure S3), but we prefer to report the actual temperature data measured at 1.5 mm of the surface. On the other hand, the Ge window is expected to give the most precise measurements compared to the ZnSe window, as it mitigates the contributions of the monolith radiance when measuring gas temperature.

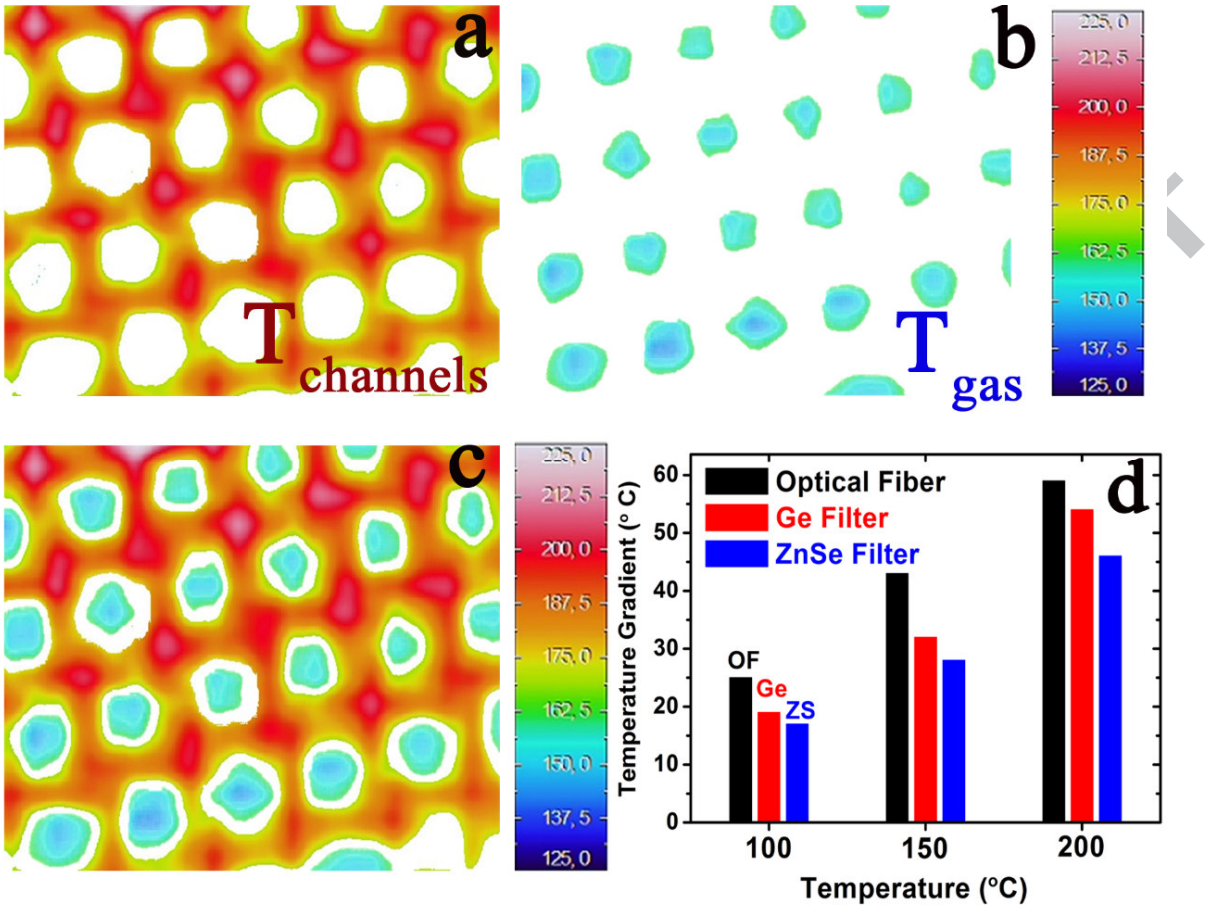

Figure 8. Images of gas an solid under reaction conditions, viewed through a Ge window. a) Close- up thermal image reconstruction of the monolith surface; b) Close-up thermal image reconstruction of the gas along the monolith channels; c) Merged thermal image reconstruction accounting for a) and b) contributions; d) Average temperature gradients between the surface of the catalyst and the gas determined by different methods.

Figure 8d shows that, indeed, stable gas-solid temperature differences can be reached in structured catalysts under microwave heating, and that these temperature gradients are very significant (higher than 50 ºC for an average catalyst temperature of 200 ºC). This may help to explain some of the results under microwave heating found in the literature. Also, the fact that it is possible to operate with a significantly lower gas temperature can be exploited to achieve improvements in reaction selectivity, when undesired secondary reactions are enhanced in a hot gas environment. Work is underway in our laboratory to study some applications of this concept.

For these studies, a precise, simultaneous measurement of gas and solid temperatures is an essential requirement.

CONCLUSIONS

The method developed in this work allows real-time measurement of gas and solid temperatures in microwave-heated structured reactors. For this purpose, a quartz vessel with suitable Ge or ZnSe windows has been designed. The algorithm developed allows, for the system used in this work, the *in-situ* determination of gas and solid emissivities, with the catalytic monolith in place, simply by taking thermal images under different modes of heating, as shown in Scheme 1. Also, in the interval explored, the weak dependency of emissivity with gas compositions in this reacting system allows to use temperature as the only relevant operation variable for emissivity. For other systems it may be necessary to correct for gas composition before obtaining accurate temperature readings. The method presented opens up new opportunities in the investigation of gas phase reactions under microwave heating. The concept has been applied to the ethylene epoxidation reaction in the presence of a MW sensitive silver-copper oxide hybrid catalyst deposited on a cordierite monolith. The presence of a gas-solid temperature gradient higher than 50 ºC has been demonstrated at a solid temperature of 200 ºC.

ACKNOWLEDGMENTS

Financial support from the European Research Council Advanced Grant (HECTOR-267626) and the Regional Government of Aragon (DGA) is gratefully acknowledged. TEM measurements were performed in the Laboratorio de Microscopias Avanzadas (LMA) at the Instituto de Nanociencia de Aragon (INA), Universidad de Zaragoza (Spain).

REFERENCES

(1) Stuerga, D. A. C., *Microwaves in Organic Synthesis (2nd Edition)*. WILEY-VCH Verlag GmbH & Co. KGaA: Weinheim, 2006.

(2) Lidström, P.; Tierney, J.; Wathey, B.; Westman, J., Microwave Assisted Organic Synthesis—a Review. *Tetrahedron* **2001,** *57* (45), 9225-9283.

(3) Kremsner, J. M.; Stadler, A.; Kappe, C. O., The Scale-up of Microwave-Assisted Organic Synthesis. In *Microwave Methods in Organic Synthesis*, Larhed, M.; Olofsson, K., Eds. 2006; Vol. 266, pp 233-278.

(4) Horikoshi, S.; Serpone, N., Role of Microwaves in Heterogeneous Catalytic Systems. *Catal. Sci. Technol.* **2014,** *4* (5), 1197-1210.

(5) Will, H.; Scholz, P.; Ondruschka, B., Microwave-Assisted Heterogeneous Gas-Phase Catalysis. *Chem. Eng. Technol.* **2004,** *27* (2), 113-122.

(6) Krech, T.; Krippendorf, R.; Jager, B.; Prager, M.; Scholz, P.; Ondruschka, B., Microwave Radiation as a Tool for Process Intensification in Exhaust Gas Treatment. *Chem. Eng. Process.* **2013,** *71*, 31-36.

(7) Durka, T.; Van Gerven, T.; Stankiewicz, A., Microwaves in Heterogeneous Gas-Phase Catalysis: Experimental and Numerical Approaches. *Chem. Eng. Technol.* **2009,** *32* (9), 1301-1312.

(8) Stankiewicz, A., On the Applications of Alternative Energy Forms and Transfer Mechanisms in Microprocessing Systems. *Ind. Eng. Chem. Res.* **2007,** *46* (12), 4232-4235.

(9) Stefanidis, G. D.; Munoz, A. N.; Sturm, G. S. J.; Stankiewicz, A., A Helicopter View of Microwave Application to Chemical Processes: Reactions, Separations, and Equipment Concepts. *Rev. Chem. Eng.* **2014,** *30* (3), 233-259.

(10) Kappe, C. O., How to Measure Reaction Temperature in Microwave-Heated Transformations. *Chem. Soc. Rev.* **2013,** *42* (12), 4977-4990.

(11) Zhang, X. L.; Hayward, D. O.; Mingos, D. M. P., Apparent Equilibrium Shifts and Hot-Spot Formation for Catalytic Reactions Induced by Microwave Dielectric Heating. *Chem. Commun.* **1999,** (11), 975-976.

(12) Kappe, C. O.; Pieber, B.; Dallinger, D., Microwave Effects in Organic Synthesis: Myth or Reality? *Angew. Chem.-Int. Edit.* **2013,** *52* (4), 1088-1094.

(13) Cecilia, R.; Kunz, U.; Turek, T., Possibilities of Process Intensification Using Microwaves Applied to Catalytic Microreactors. *Chem. Eng. Process.* **2007,** *46* (9), 870-881.

(14) Horikoshi, S.; Kamata, M.; Mitani, T.; Serpone, N., Control of Microwave-Generated Hot Spots. 6. Generation of Hot Spots in Dispersed Catalyst Particulates and Factors That Affect Catalyzed Organic Syntheses in Heterogeneous Media. *Ind. Eng. Chem. Res.* **2014,** *53* (39), 14941-14947.

(15) Zhang, X. L.; Hayward, D. O., Applications of Microwave Dielectric Heating in Environment-Related Heterogeneous Gas-Phase Catalytic Systems. *Inorg. Chim. Acta* **2006,** *359* (11), 3421-3433.

(16) Durka, T.; Stefanidis, G. D.; Van Gerven, T.; Stankiewicz, A., On the Accuracy and Reproducibility of Fiber Optic (Fo) and Infrared (Ir) Temperature Measurements of Solid Materials in Microwave Applications. *Meas. Sci. Technol.* **2010,** *21* (4).

(17) Will, H.; Scholz, P.; Ondruschka, B., Heterogeneous Gas-Phase Catalysis under Microwave Irradiation - a New Multi-Mode Microwave Applicator. *Top. Catal.* **2004,** *29* (3-4), 175-182.

(18) Gracia, J.; Escuin, M.; Mallada, R.; Navascues, N.; Santamaria, J., Nano-Heaters: New Insights on the Outstanding Deposition of Dielectric Energy on Perovskite Nanoparticles. *Nano Energy* **2016,** *20*, 20-28.

(19) Ramirez, A.; Hueso, J. L.; Mallada, R.; Santamaria, J., Ethylene Epoxidation in Microwave Heated Structured Reactors. *Catal. Today* **2016,** *273*, 99-105.

(20) Zhang, J. S.; Zhang, C. Y.; Liu, G. T.; Luo, G. S., Measuring Enthalpy of Fast Exothermal Reaction with Infrared Thermography in a Microreactor. *Chem. Eng. J.* **2016,** *295*, 384-390.

(21) Haber, J.; Kashid, M. N.; Borhani, N.; Thome, J.; Krtschil, U.; Renken, A.; Kiwi-Minsker, L., Infrared Imaging of Temperature Profiles in Microreactors for Fast and Exothermic Reactions. *Chem. Eng. J.* **2013,** *214*, 97-105.

(22) Safitri, A.; Mannan, M. S., Methane Gas Visualization Using Infrared Imaging System and Evaluation of Temperature Dependence of Methane Gas Emissivity. *Ind. Eng. Chem. Res.* **2010,** *49* (8), 3926-3935.

(23) Hodgkinson, J.; Tatam, R. P., Optical Gas Sensing: A Review. *Measurement Science and Technology* **2013,** *24* (1).

(24) Welty, J.; Wicks, C. E.; Rorrer, G. L.; Wilson, R. E., *Fundamentals of Momentum, Heat and Mass Transfer*. Willey: New York, 2008.

(25) Ramirez, A.; Hueso, J. L.; Suarez, H.; Mallada, R.; Ibarra, A.; Irusta, S.; Santamaria, J., A Nanoarchitecture Based on Silver and Copper Oxide with an Exceptional Response in the Chlorine-Promoted Epoxidation of Ethylene. *Angew. Chem. Int.Ed.* **2016,** *55* (37), 11158-11161.

(26) Shen, X. M.; Xu, G. Y.; Shao, C. M.; Cheng, C. W., Temperature Dependence of Infrared Emissivity of Doped Manganese Oxides in Different Wavebands (3-5 and 8-14 Mu M). *J. Alloy. Compd.* **2009,** *479* (1-2), 420-422.

(27) http://webbook.nist.gov/cgi/cbook.cgi?ID=C74851&Type=IR-SPEC&Index=6#IR-SPEC.

(28) Hottel, H. C.; Sarofim, A. F., Models of Radiative Transfer in Furnaces. *J. Eng. Phys. Thermophys.* **1970,** *19* (3), 1102-1114.

(29) Goody, R. M., A Statistical Model for Water-Vapour Absorption. *Q. J. R. Meteorol. Soc.* **1952,** *78* (336), 165-169.

(30) Danjoux, R., *Infrared Training Center, Technical Publication Number T560472_A-en-US.*

(31) Huang, R. S.; Liu, L. M.; Song, G., Infrared Temperature Measurement and Interference Analysis of Magnesium Alloys in Hybrid Laser-Tig Welding Process. *Mater. Sci. Eng. A-Struct. Mater. Prop. Microstruct. Process.* **2007,** *447* (1-2), 239-243.

(32) Vollmer, M.; Mollmann, K.-P., *Infrared Thermal Imaging: Fundamentals, Research and Applications*. Wiley 2010.

Highlights

- Determination of gas-solid temperature gradients under microwave heating.
- Custom-designed vessel for direct observation of the catalysts under reaction.
- Preferential heating on microwave-absorbing catalyst surface is observed.
- Infrared thermography coupled with optical fibers provides essential information for temperature evaluation.

GRAPHICAL ABSTRACT

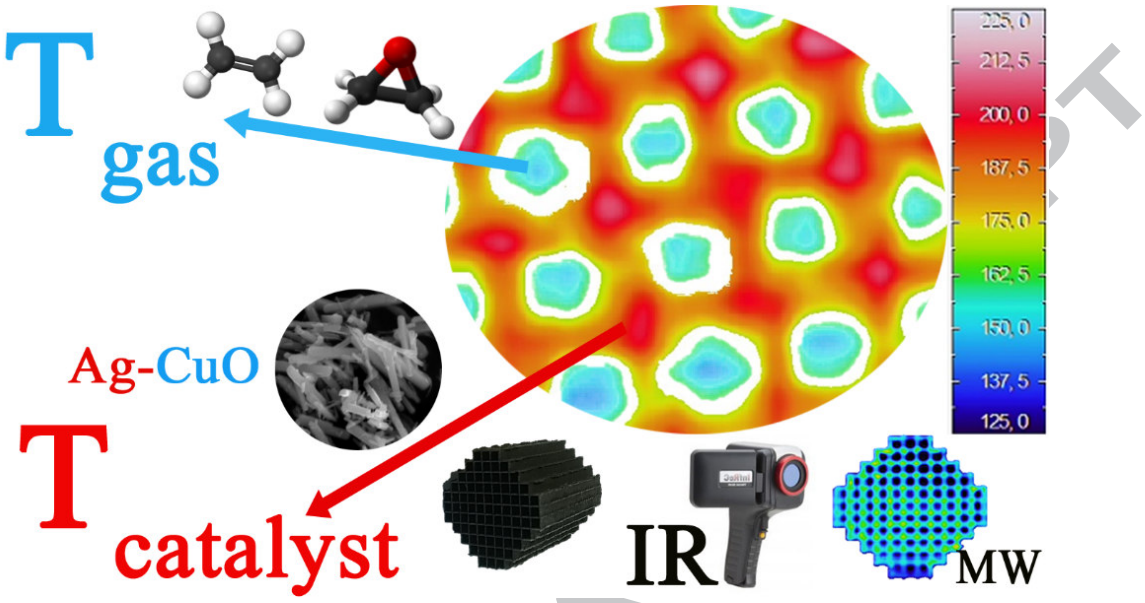

Development and optimization of a method for an accurate, real-time measurement of gas-solid temperature gradients in microwave-heated structured reactors using infrared thermometry